This is a repository copy of *Solar evaporation via nanofluids: A comparative study*.

White Rose Research Online URL for this paper:
http://eprints.whiterose.ac.uk/133619/

Version: Accepted Version

Solar evaporation via nanofluids: A comparative study

Aimen Zeiny[a, c] *, Haichaun Jin[b], Guiping Lin[b], Pengxiang Song, Dongsheng Wen[b, a] *

[a] School of Chemical and Process Engineering, University of Leeds, Leeds, LS2 9JT, UK

[b] School of Aeronautic Science and Engineering, Beihang University, Beijing PR China

[c] Department of Mechanical Engineering, University of Kufa, Najaf, Iraq

Tel: +44 113 3431299

* Corresponding authors and E-mails: D.Wen@leeds.ac.uk ; ml12arnz@leeds.ac.uk

Abstract: Vaporisation (evaporation and boiling) through direct volumetric solar collectors has recently drawn significant attention. Many studies suggested plasmonic nanoparticles, such as gold nanoparticles, to significantly enhance the photo-thermal conversion efficiency. However, there is still a lack of comparative studies of the feasibility of using gold nanoparticles for solar applications. This study performed well-controlled experiments for two different categorised particles, i.e., gold and carbon black suspended in water, and assessed their performance in terms of evaporation rate, materials cost and energy consumption. The results show that gold nanofluids are not feasible for solar evaporation applications, where the cost of producing 1g/s vapour is ~300 folds higher than that produced by carbon black nanofluids. This infeasibility is mainly due to the high cost and the low absorbance of gold comparing to carbon black nanoparticles. Moreover, this work reveals that the higher the nanoparticles concentration and/or the incident solar radiation is, more energy is trapped in a small volume of the nanofluid near the interface, resulting in a higher temperature near the interface and a higher evaporation rate. Future optimization of the system should consider concentrating more solar energy at the surface to allow the maximum amount of solar is used for evaporation.

Keywords: Direct absorption, nanofluid, nanoparticle, solar energy, solar evaporation.

1. Introduction

Efficient renewable energy conversion technologies are critically essential to address the environment pollution, fossil fuel depletion and population increase problems. Solar energy, as one of the renewable energy resources, has been claimed as the energy of our future. However, challenges such as high cost (due to using optical devices such as heliostats or reflectors to concentrate the solar energy, tracking devices to track the energy source, and vast land for installation) and low efficiency (due to the heat losses) of the solar energy conversion systems [1-3] limit its wide applications.

Nanoparticle-based direct absorption solar energy collectors (DASCs), which utilize the high radiation absorption property of nanoparticles suspended in a working fluid, are a method to increase the efficiency of solar systems. Since the proposition of this method, enormous efforts have been done to investigate the effects of nanoparticles' composition, size, and shape on the photo-thermal conversion efficiency of the DASCs [1, 2, 4-25].

Recently, DASCs have been proposed as novel solar-driven steam generation systems [3], and using gold nanoparticle has attracted intense interest [4, 7, 10, 12, 13, 17, 19, 25-28], albeit it is one of the most expensive materials. This interest comes from two main reasons: Firstly,most of the solar working fluids are semi-transparent for the visible spectrum, which represents ~40% of the solar energy, and the resonance of the conducting electrons of the gold nanoparticles can be tuned so that the peak absorbance occurs in the visible spectrum. As the enhancement in the light absorption has unavoidably a narrow bandwidth of the wavelength [7], this promotes the use of hybrids of different sizes and/or shapes of gold nanoparticles to broaden the bandwidth of the peak absorption [7, 13, 19, 25]. However, a reduction in the peak absorption value necessarily occurs due to the dilution of gold nanofluids at a given total particle concentration, according to the Beer's law. This means a higher concentration of gold nanoparticles is needed to prepare a hybrid with a broad bandwidth at the same peak value of absorbance. Secondly, the claim of nanobubbles generation around immersed nanoparticles can enhance the efficiency

of the solar-driven steam generation, albeit the bulk temperature of a nanofluid still subcooled [17, 29, 30]，is still subjecting to strong debate. It has been suggested that nanobubbles can only be generated under very high intensity of light, i.e., of thousands of kW/m^2 [5, 31-33], which consequently requires expensive optical and tracking devices.

Many studies assumed a uniform temperature distribution within a nanofluid although the effect of the optical path was not negligible, and one temperature was used to analyse the photo-thermal conversion efficiency [11, 14-17, 28, 30]. However, the non-linearly reduction in the radiative intensity along the depth of the nanofluid should cause large temperature difference within the nanofluid [5, 6]. Neglecting this temperature difference will lead to an inaccurate analysis of the results. Moreover, most of the published work was based on only one particular type of particles, and a comparative assessment of the performance of commonly used nanomaterials for solar-driven steam generation is still lacking. The effect of these nanomaterials needs to be investigated at the same concentration and under similar operating conditions to reach a fair comparison [3]. In addition to the efficiency, the cost must be considered very carefully for any practical application. For the purpose of comparison, some estimation of the cost of a unit steam generation rate ($/g/s) from different nanoparticles is preferred.

This study aims to clarify the mechanism of the solar steam generation and to investigate the feasibility of using gold nanoparticles under low concentrations of solar radiation. By performing well-controlled experiments, a comparison between aqueous gold (Au) and carbon black (CB) nanofluids were conducted. Evaporation rate, cost of a unit steam rate generation ($/g/s), and energy consumption were calculated from the recorded transient temperature rise and mass change. Furthermore, more experiments were conducted to investigate the effect of the incident solar radiation intensity on the temperature distribution within the nanofluids.

2. Preparation of nanofluids
2.1. Synthesis of gold nanofluid

In this study, gold nanofluid (Au) was synthesised by the citrate reduction method as reported by Chen and Wen [34] and Zhang et. al [12]. Typically, 100 ml of 5 mM $HAuCl_4$ solution was mixed with 100 ml of 10 mM tri-sodium citrate solution. Then, the resultant mixture was heated to the boiling temperature until its colour became wine red. After that, the resultant was put into a sonication bath at $80^{o}C$ for 3 hours. The synthesised gold nanoparticles were left for 24 hours at the room temperature and then purified by the membrane dialysis method. In this process, the gold nanofluid was put in a membrane tube with a pore size of 2-3 nm in diameter to allow a smooth diffusion of ions and keep the gold nanoparticles inside the tube. The membrane tube was placed in a beaker filled with DI water of 2000 ml and stirred by a magnetic stirrer. The DI water was changed twice a day for ten days.

2.2. Preparation of carbon black nanofluid

Carbon black (CB) nanofluid was prepared by the two-step method, i.e. by dispersing a certain amount of pre-synthesised nanopowder to a hosting liquid, i.e., deionized (DI) water in this work. The carbon black nanopowder was purchased from Alfa Aesar. The dispersing agent of Tween was added to DI water at 0.04 vol. %. The hosting liquid was magnetically stirred when controlled amount of nanopowder was added. After 15 minutes, the sample was put into an ultrasonication bath for 30 minutes, followed by a powerful probe sonicator for extra 30 minutes.

3. Characterisation

A flame atomic absorption spectrometer (AAS) was used to measure the concentration of the prepared gold nanofluid, which turned out to be 250 mg/l. Different dilutions (25, 50, and 100 mg/l) were prepared from the stock nanofluids (see Figure 1). UV-Vis Spectrophotometer (UV-1800, SHIMADZU) was used to measure the capability of radiation absorption of gold and carbon black dilutions. The absorption spectra are shown in Figure 2 (A) and 3 (A) respectively. The results reveal an excellent agreement between the absorbance results and the Beer's law, which indicates a linear relationship between absorbance and solution concentration, as shown in the insets of the two figures. The slope of the absorbance line of the

gold nanofluids is $0.01\frac{1/cm}{mg/l}$, while it is $0.029\frac{1/cm}{mg/l}$ for the carbon black nanofluids. It is clear that gold nanofluids have good absorbance in the range of 300-600 nm wavelength and the peak value is around 528 nm, which is due to the local surface plasmon resonance. However, the absorption capability of the carbon black nanofluids is better than the gold nanofluids over the measuring spectrum. Moreover, the zeta-potential and nanoparticle size distribution were measured by a zetasizer (Malvern). The zeta-potentials were (-37.6 mV) and (-32.3 mV), and the size distributions are shown in Figure 2 (B) and 3 (B) for gold and carbon black nanofluids respectively.

4. Solar evaporation experimental setup

The photo-thermal conversion experimental setup is shown in Figure 4. A solar simulator (ORIEL® Sol3A™ CLASS AAA SOLAR SIMULATOR) was used as a light source to minimise the uncertainties under direct sunlight. This solar simulator provides a radiation spectrum match the solar spectra, and the intensity can be varied by using suitable filters. This device is certified to IEC 60904-9 2007 edition, JIS C 8912 and ASTM E 927-05 standards. The performance parameters of the sun simulator are; non-uniformity < 2% and temporal instability < 0.5%. A FLIR ONE infrared camera (sensitivity of 0.1 °C) to detect the temperature distribution within the nanofluids, a Fresnel lens (Edmund Optics) with a 250 mm focal distance to focus the source light, and a digital weighing scale (Ohaus Discovery, a precision of ±0.1 mg) to measure the samples' mass change were used.

Two containers were utilised in this study: a cylindrical one of 35 mm diameter and 40 mm height was used to get the temperature distribution within the nanofluids using the infrared camera, and the other one was a Petri dish of 35 mm diameter. By using precise micro-pipettes, 45 ml sample was put in the cylindrical container, and a 4 ml sample was put in the Petri dish to form a thin layer of the nanofluid (~4 mm) to minimise the temperature gradient within the sample. The Petri dish was placed on the bottom of an upside down glass beaker in the centre spot of the solar simulator. A K-type thermocouple (Omega 5TC-TT-K-36-36, a precision of ±0.5 °C) was used

to measure the temperature of the centre of the sample. The transient data (mass and bulk temperature) was recorded to a PC via a data acquisition system under the LabVIEW environment. Preliminary tests with five thermocouples located at different positions on the bottom of the Petri dish showed that the space variation of the sample temperature was negligible.

5. Results and discussion

5.1. Experiment with 45 ml samples

To demonstrate the effect of nanoparticles on the solar radiation absorption, temperature distribution within the bulk fluid and evaporation rate, experiment was done by using gold nanofluids (0, 25, 50, 100 mg/l) subjected to a radiation (heating-up) from a solar simulator (10 kW/m^2) for 900 s and continued for another 900 s without radiation (cooling-down). A FLIR ONE infrared thermal camera (0.1°C sensitivity) was used to capture the temperature distribution within the nanofluid's depth each 60 s and a precise mass scale (0.1 mg sensitivity) was used to measure the mass change each second. The results are shown in Table 1 and Figure 5. It is clear that adding nanoparticles to water makes the temperature distribution highly non-homogeneous. With the increase of nanoparticle concentration, the hottest layer of the nanofluid becomes thinner and closer to the interface between the gaseous and liquid phases, resulting in a higher evaporation rate. Also, it is clear that a thin layer of nanofluid is needed to minimise the nonhomogeneity in the temperature. Therefore, a small volume of the nanofluids was used to investigate the feasibility of using gold nanofluids in solar evaporation applications, as below.

5.2. Experiment with 4 ml samples

In this experiment, a 4 ml of gold or carbon black nanofluid sample was put in the 35 mm Petri dish making ~4 mm thin layer under a solar radiation of 10 kW/m^2 for 600 s. During this period, the samples' temperature and mass were recorded, as shown in Figure 6. It is evident that the temperature and mass change trends are the same for both carbon black and gold nanofluids. Only the values are different, and this depends on the light absorption characteristics. Both the temperature and the evaporated mass of the carbon black nanofluids are higher than that of

gold nanofluid, which is consistent with the absorbance characteristics shown in Figure 2 (A) and Figure 3 (A).

Figure 7 shows the evaporation rate, the numerical differentiation of the mass change with time, as a function of time and temperature for gold and carbon black nanofluids respectively. It is noted that for both samples, the evaporation rate of a nanofluid is higher during the heating-up period than the cooling-down period at the same temperature. This shall be related to the surface temperature difference between the heating and cooling period. It shall be noted that he thermocouple is located 2 mm beneath the surface. Although the measued fluid temperature is the same, the surface temperature during the heating shall be higher than that during the cooling. As the evaporation rate is proportional to the kinetic energy of the water molecules at the interface between the gasous and liquid phases, a higher evaporation rate is expected during the heating period.

In addition, one can see that the evaporation rate of different nanofluid concentrations is the same during the cooling-down period at temperatures below 35°C. This is consistent with the temperature measurement in Figure 6 where the temperatures of all concentrations become the same after time ~1100 s. As a result, one can say that the effect of the nanoparticles is just to enhance the radiation absorption properties. To enhance the evaporation rate, a better approach is to trap most of the solar energy near the surface, which requires very high nanoparticle concentrations. That will raise problems such as nanoparticles' instability, viscosity increase, and cost increase.

To investigate the feasibility of using gold nanofluids in solar evaporation applications, the cost of producing 1 g/s of water vapour was calculated as:

$$Cost \left[\frac{\$}{\frac{g}{s}} \right] = \frac{Cost_{np} [\frac{\$}{g}]}{\frac{\dot{m} [\frac{g}{s}]}{V [ml] * C [\frac{mg}{l}]}} 10^6 \qquad (1)$$

where $Cost_{np}$ is the cost of 1 gram of the nanoparticles. $43 was used for gold nanoparticles, which represents the price of gold in the global stocks market, and $0.18 was used for carbon black nanoparticles, which represents the supplier price; $\dot{m}$ is the evaporation rate; V is sample's volume and C is the sample's concentration. The results are shown in Figure 8. The cost of producing 1 g/s vapour by gold nanofluids is much higher than that produced by carbon black nanofluids (~300 folds). Also, one can see that the cost of producing vapour is proportional to the nanoparticles concentration even though the evaporation rate increases as the concentration increases. This is because most of the nanoparticles are in the bulk volume of the samples and not directly participate in vapour production.

The following equations were used to investigate how much of the absorbed solar energy was consumed for evaporation and how much was for heating-up the bulk nanofluid:

$$E_{evap.} = \Delta m \ [g] * h_{fg} \ [\frac{J}{g}] \tag{2}$$

$$E_{heating-up} = C_p \left[\frac{J}{gK}\right] * m \ [g] * \Delta T \ [K] \tag{3}$$

where;

$E_{evap.}$ is energy consumed by evaporation,

Δm is mass of vapour,

h_{fg} is enthalpy change from liquid to vapour,

$E_{heating-up}$ is energy stored in the nanofluid,

C_p is the specific heat capacity of the nanofluid ~ of water,

m is the sample mass,

ΔT is the temperature change.

The results are shown in Figure 9 and Figure 10 respectively. It is clear that the energy used for evaporation by carbon black nanofluids is ~1.5 times higher than that consumed by gold nanofluids. The latent to sensible heat ratio is also higher for carbon black nanofluids, and such a ratio increases as the concentration increases.

6. Conclusions

This work investigated the evaporation mechanism of aqueous gold and carbon black nanofluids subjecting to concentrated solar radiation. Experiments were conducted using a AAA-rated solar simulator to minimise the uncertainties accompanied with the natural solar radiation. It was found that:

- The higher the concentration of the nanoparticles and/or the higher the incident light intensity is, the more of the solar energy is trapped in a slim volume near the air-nanofluid interface, leading to a higher interface temperature, and consequently higher evaporation rate. This trend is consistent with the Beer's law, which indicates that the absorbed radiation energy is an exponential function of the extinction coefficient, which is a function of the nanoperticles concentration, and light path length.

- The higher the concentration of the nanoparticles is, the higher ratio of the energy consumed for evaporation to the energy stored in a nanofluid is.

- To enhance the solar evaporation rate, higher nanoparticle concentrations are required to trap most of the solar energy in a very thin layer. This will raise many problems such as the instability of the nanoparticles, the change of the physio-thermal properties of the nanofluids, and the high cost as the most of the nanoparticles are in the bulk volume and do not participate in the evaporation enhancement directly.

- Moreover, this work revealed that gold nanofluids are not feasible for solar evaporation applications due to the high cost and low radiation absorbance especially for the wavelength after 600 nm. While carbon black nanofluids are cheaper and more efficient than gold nanofluids.

References

1.	Otanicar, T.P., et al., *Nanofluid-based direct absorption solar collector.* Journal of renewable and sustainable energy, 2010. **2**(3): p. 033102.

2.	Gupta, H.K., G.D. Agrawal, and J. Mathur, *An experimental investigation of a low temperature Al 2 O 3-H 2 O nanofluid based direct absorption solar collector.* Solar Energy, 2015. **118**: p. 390-396.

3.	Deng, Z., et al., *An emergence of solar thermal utilization: solar-driven steam generation.* Journal of Materials Chemistry A, 2017.

4.	Fu, Y., et al., *Investigation on enhancing effects of Au nanoparticles on solar steam generation in graphene oxide nanofluids.* Applied Thermal Engineering, 2017. **114**: p. 961-968.

5.	Jin, H., et al., *Steam generation in a nanoparticle-based solar receiver.* Nano Energy, 2016. **28**: p. 397-406.

6.	Jin, H., et al., *Photothermal conversion efficiency of nanofluids: An experimental and numerical study.* Solar Energy, 2016. **139**: p. 278-289.

7.	Jeon, J., S. Park, and B.J. Lee, *Analysis on the performance of a flat-plate volumetric solar collector using blended plasmonic nanofluid.* Solar Energy, 2016. **132**: p. 247-256.

8.	Ishii, S., R.P. Sugavaneshwar, and T. Nagao, *Titanium nitride nanoparticles as plasmonic solar heat transducers.* The Journal of Physical Chemistry C, 2016. **120**(4): p. 2343-2348.

9.	Ishii, S., et al., *Solar water heating and vaporization with silicon nanoparticles at Mie resonances.* Optical Materials Express, 2016. **6**(2): p. 640-648.

10.	Zhang, H., et al., *Dependence of Photothermal Conversion Characteristics on Different Nanoparticle Dispersions.* Journal of Nanoscience and Nanotechnology, 2015. **15**(4): p. 3055-3060.

11.	Chen, M., et al., *An experimental investigation on sunlight absorption characteristics of silver nanofluids.* Solar Energy, 2015. **115**: p. 85-94.

12.	Zhang, H., et al., *Photothermal conversion characteristics of gold nanoparticle dispersions.* Solar Energy, 2014. **100**: p. 141-147.

13.	Jeon, J., S. Park, and B.J. Lee, *Optical property of blended plasmonic nanofluid based on gold nanorods.* Optics express, 2014. **22**(104): p. A1101-A1111.

14. Bandarra Filho, E.P., et al., *Experimental investigation of a silver nanoparticle-based direct absorption solar thermal system.* Energy Conversion and Management, 2014. **84**: p. 261-267.

15. He, Q., et al., *Experimental investigation on photothermal properties of nanofluids for direct absorption solar thermal energy systems.* Energy Conversion and Management, 2013. **73**: p. 150-157.

16. Yousefi, T., et al., *An experimental investigation on the effect of Al 2 O 3–H 2 O nanofluid on the efficiency of flat-plate solar collectors.* Renewable Energy, 2012. **39**(1): p. 293-298.

17. Neumann, O., et al., *Solar vapor generation enabled by nanoparticles.* Acs Nano, 2012. **7**(1): p. 42-49.

18. Lenert, A. and E.N. Wang, *Optimization of nanofluid volumetric receivers for solar thermal energy conversion.* Solar Energy, 2012. **86**(1): p. 253-265.

19. Lee, B.J., et al., *Radiative heat transfer analysis in plasmonic nanofluids for direct solar thermal absorption.* Journal of solar energy engineering, 2012. **134**(2): p. 021009.

20. Khullar, V., et al., *Solar energy harvesting using nanofluids-based concentrating solar collector.* Journal of Nanotechnology in Engineering and Medicine, 2012. **3**(3): p. 031003.

21. Taylor, R.A., et al., *Nanofluid optical property characterization: towards efficient direct absorption solar collectors.* Nanoscale research letters, 2011. **6**(1): p. 1-11.

22. Sani, E., et al., *Potential of carbon nanohorn-based suspensions for solar thermal collectors.* Solar Energy Materials and Solar Cells, 2011. **95**(11): p. 2994-3000.

23. Mercatelli, L., et al., *Absorption and scattering properties of carbon nanohorn-based nanofluids for direct sunlight absorbers.* Nanoscale research letters, 2011. **6**(1): p. 1-9.

24. Sani, E., et al., *Carbon nanohorns-based nanofluids as direct sunlight absorbers.* Optics Express, 2010. **18**(5): p. 5179-5187.

25. Cole, J.R. and N. Halas, *Optimized plasmonic nanoparticle distributions for solar spectrum harvesting.* Applied physics letters, 2006. **89**(15): p. 153120.

26. Zhou, L., et al., *Self-assembly of highly efficient, broadband plasmonic absorbers for solar steam generation.* Science advances, 2016. **2**(4): p. e1501227.

27. Bae, K., et al., *Flexible thin-film black gold membranes with ultrabroadband plasmonic nanofocusing for efficient solar vapour generation.* Nature communications, 2015. **6**.

28.   Neumann, O., et al., *Combining Solar Steam Processing and Solar Distillation for Fully Off-Grid Production of Cellulosic Bioethanol.* ACS Energy Letters, 2016. **2**: p. 8-13.

29.   Polman, A., *Solar steam nanobubbles.* ACS nano, 2013. **7**(1): p. 15-18.

30.   Neumann, O., et al., *Compact solar autoclave based on steam generation using broadband light-harvesting nanoparticles.* Proceedings of the National Academy of Sciences, 2013. **110**(29): p. 11677-11681.

31.   Baffou, G., et al., *Super-heating and micro-bubble generation around plasmonic nanoparticles under cw illumination.* The Journal of Physical Chemistry C, 2014. **118**(9): p. 4890-4898.

32.   Boriskina, S.V., H. Ghasemi, and G. Chen, *Plasmonic materials for energy: From physics to applications.* Materials Today, 2013. **16**(10): p. 375-386.

33.   Phelan;, P.F., et al., *Light-Induced Energy Conversion in Liquid Nanoparticle Suspensions*, in *NANOPARTICLE HEAT TRANSFER AND FLUID FLOW*, W.J.M.E.M.S.J.P. Abraham, Editor. 2013, CRC Press, Taylor & Francis Group.

34.   Chen, H.-J. and D. Wen, *Ultrasonic-aided fabrication of gold nanofluids.* Nanoscale research letters, 2011. **6**(1): p. 1-8.
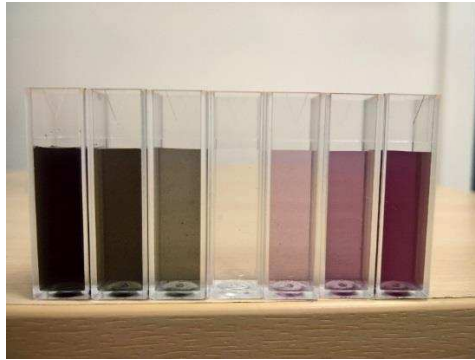
Figure 1: Picture of gold and carbon black nanofluid dilutions. The mid sample is DI water, to the right are gold nanofluids and to the left are carbon black nanofluids. The concentrations are 25, 50, and 100 mg/l respectively.
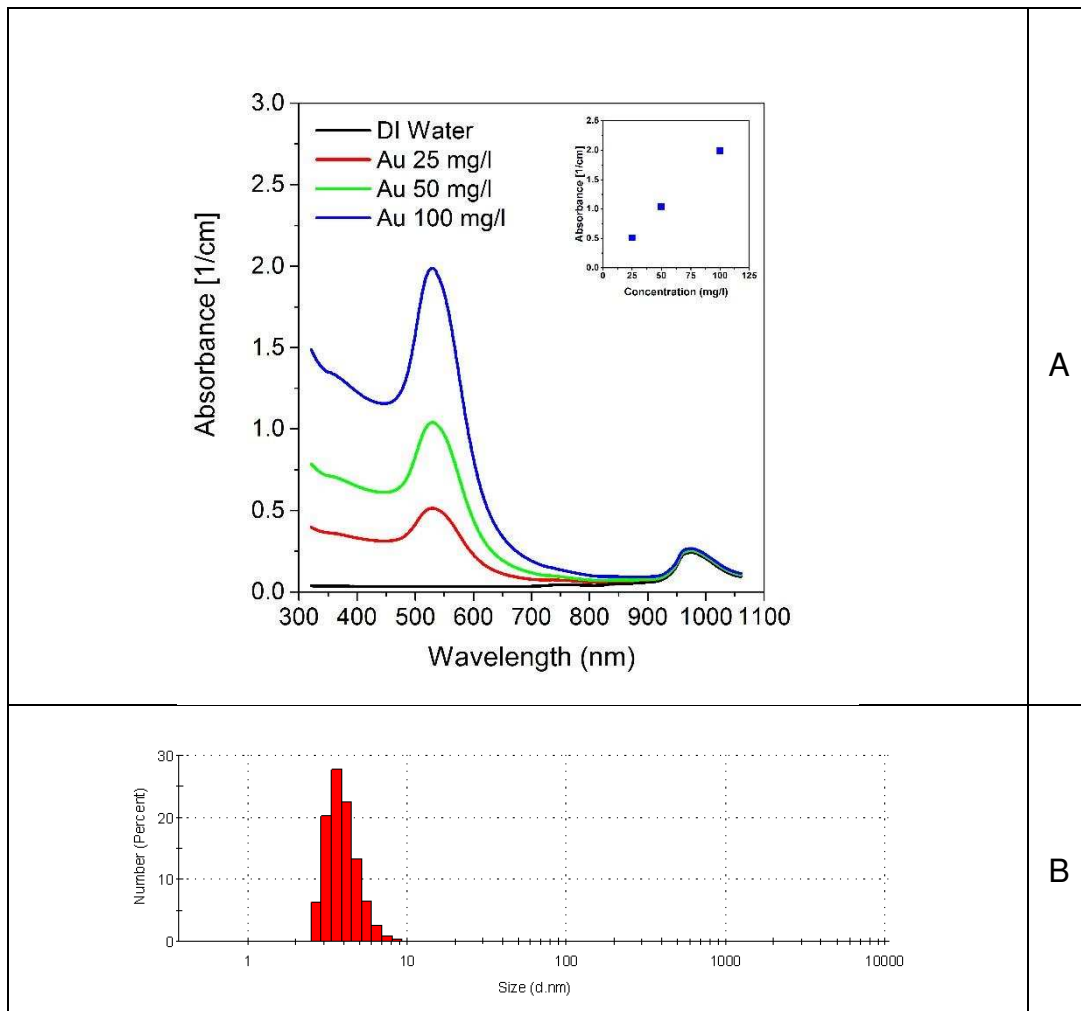

Figure 2: Spectrum absorbance (A), and the particle size distribution (B) of gold nanofluids.
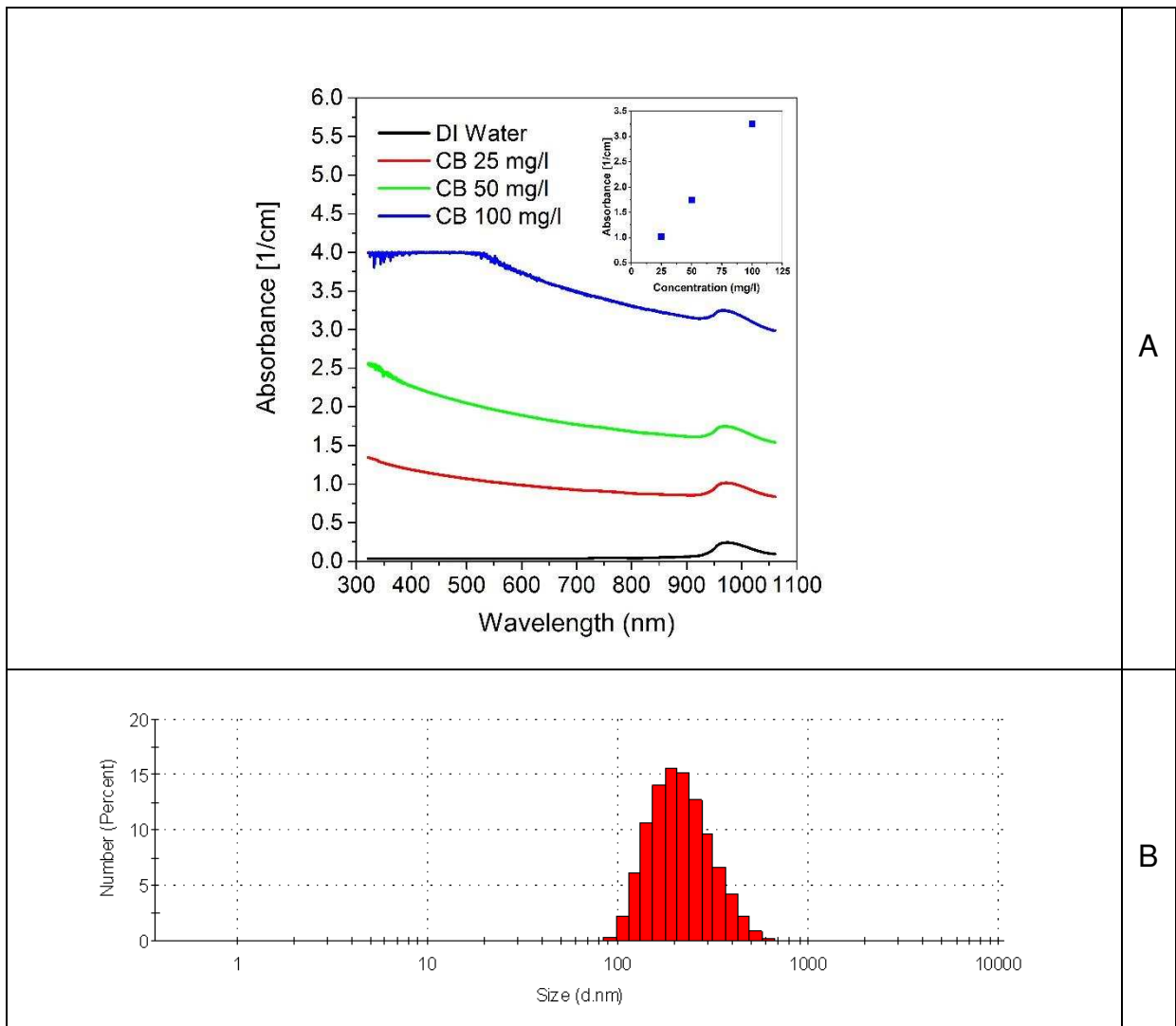
**Figure 3: Spectrum absorbance (A), and the particle size distribution (B) of carbon black nanofluids.**
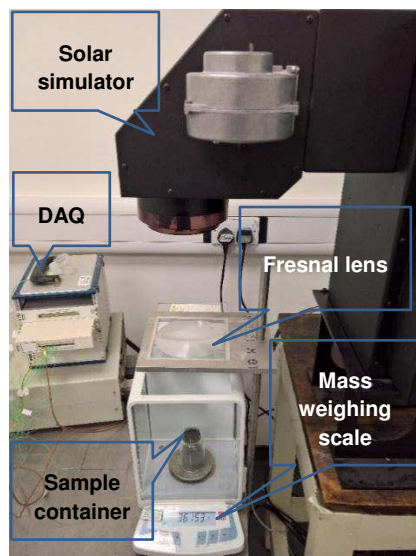
Figure 4: Solar evaporation experimental setup.

Table 1: Temperature distribution within different concentration of gold nanofluids. The samples are subjected to 10 kW/m^2 radiation for the first 15 min (heating-up process), after that samples go through a cooling-down process (No radiation).
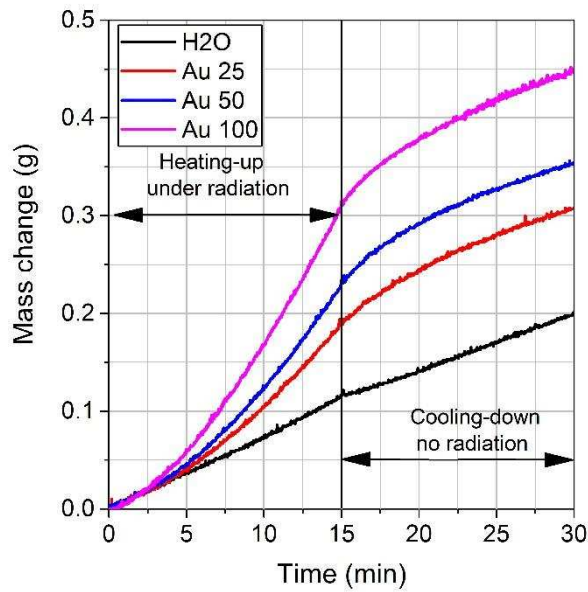
Figure 5: The temporary mass change of different concentrations of gold nanofluids.

| A | B |
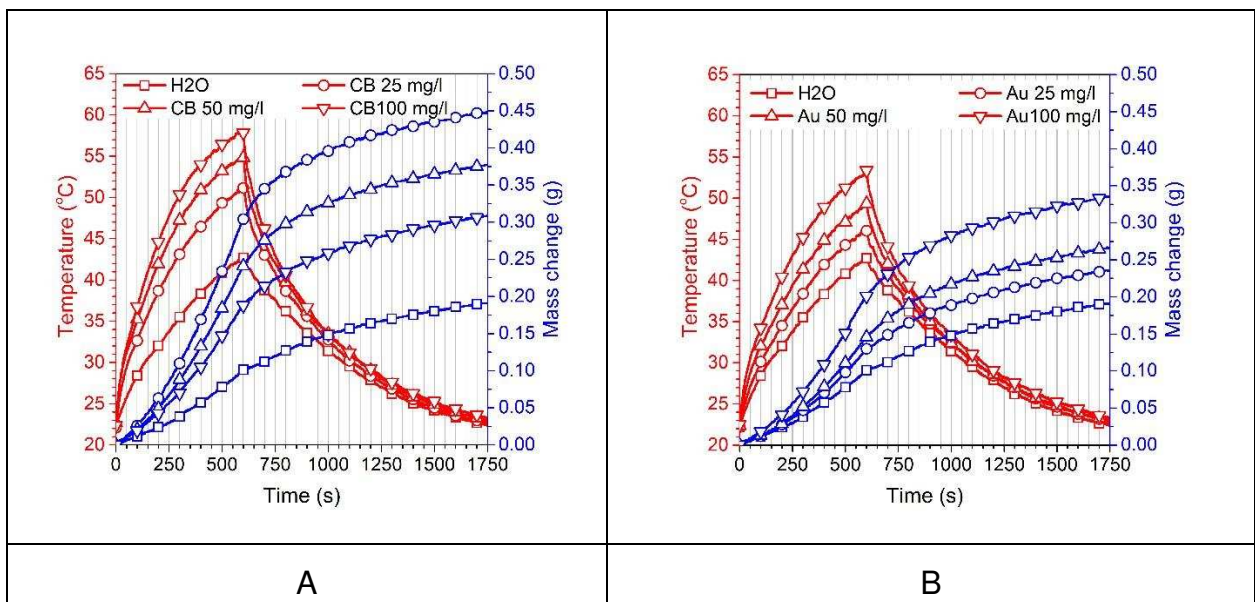
**Figure 6: Transient temperature and mass change for (A) carbon black and (B) Gold nanofluids.**
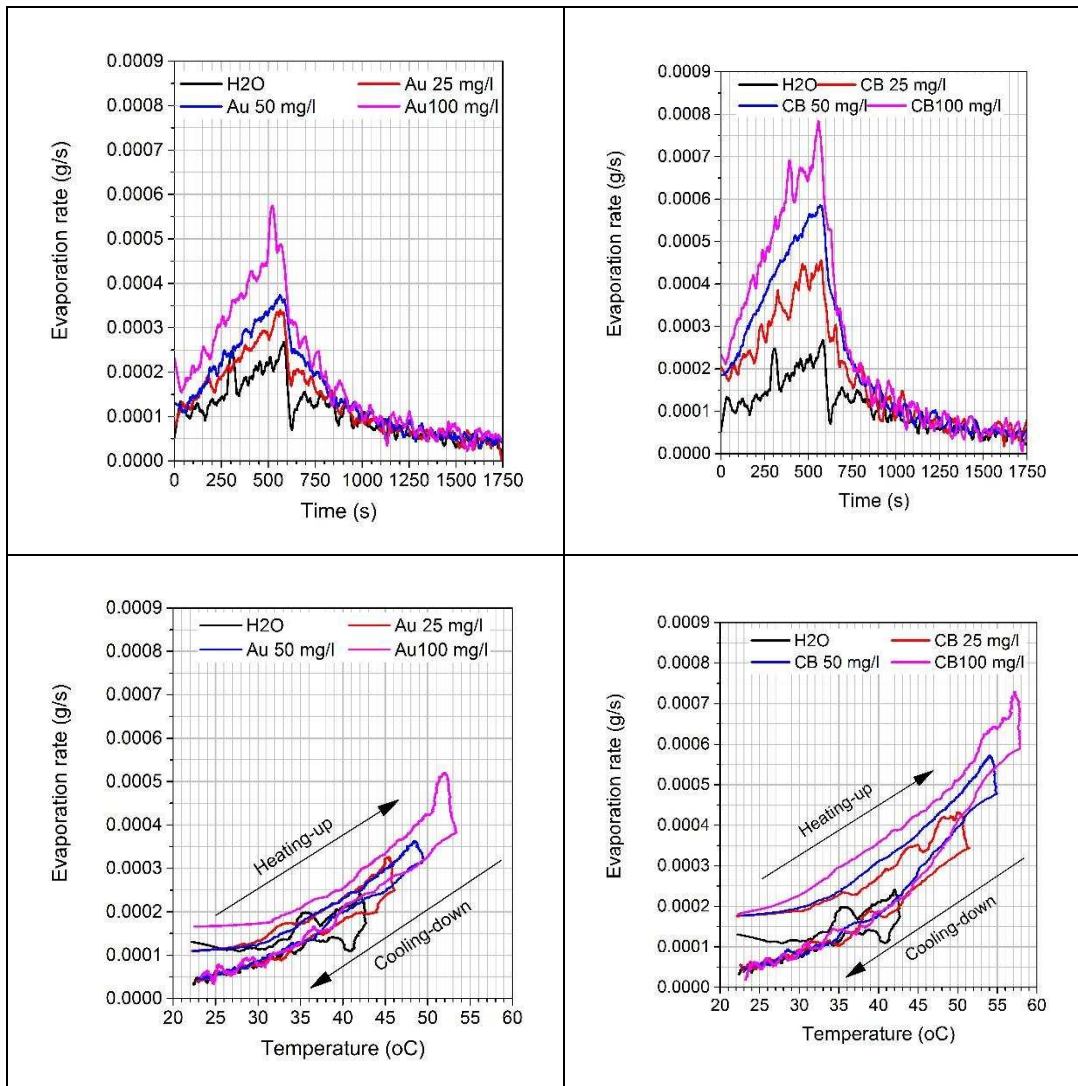
Figure 7: Evaporation rate for Gold and carbon black nanofluids as function of time and temperature respectively.
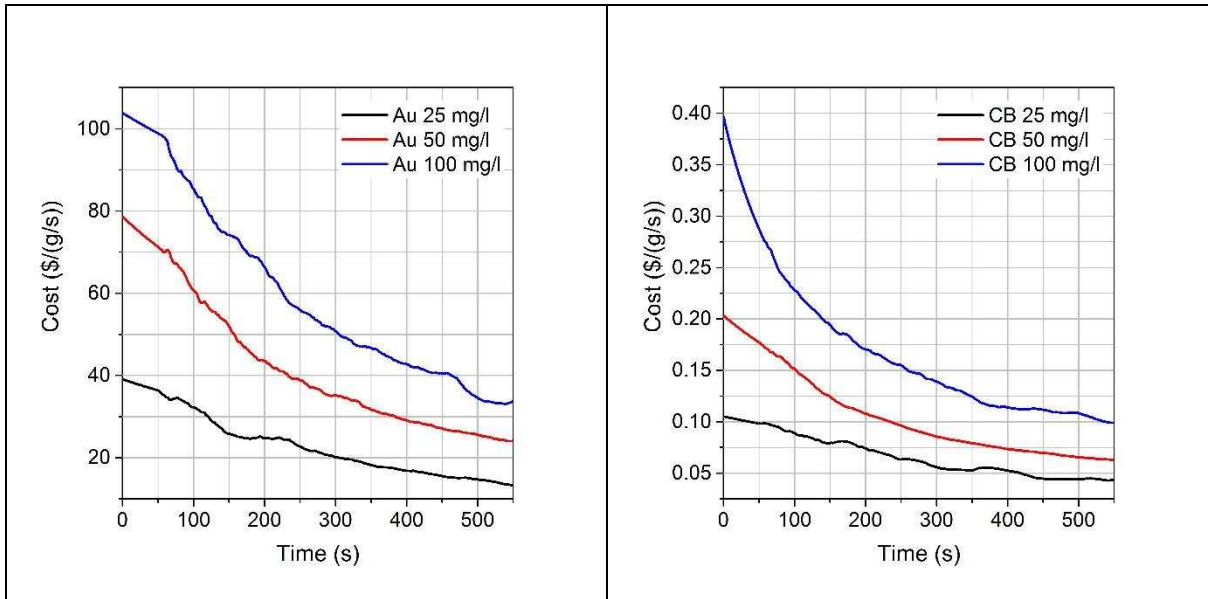
Figure 8: The transient cost of producing 1 g/s vapour using gold and carbon black nanofluids.
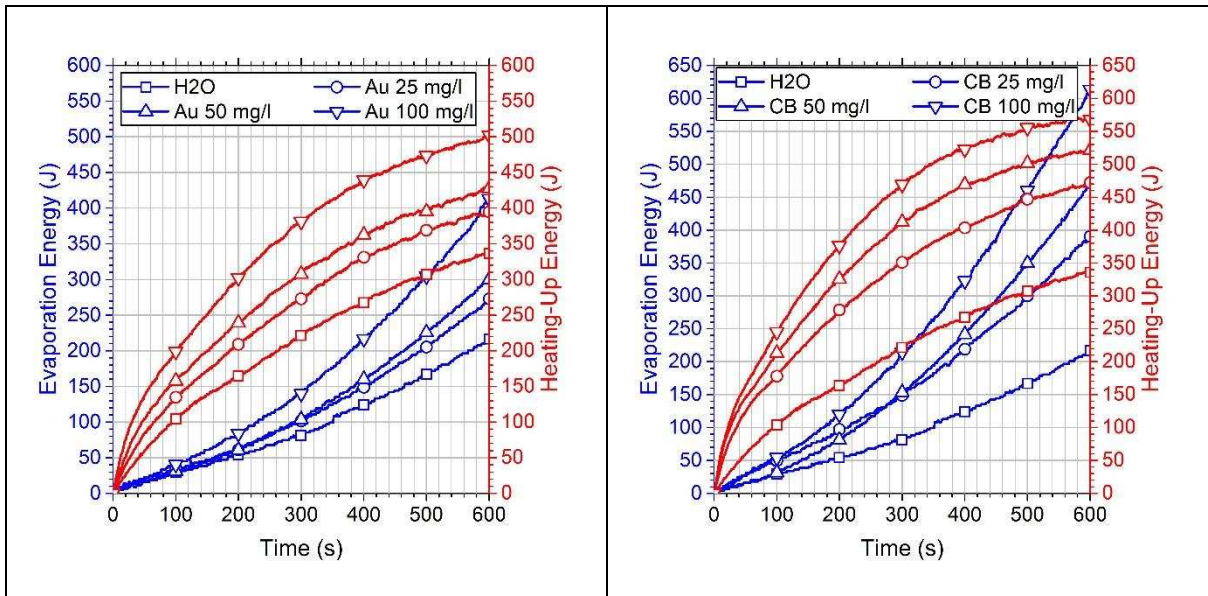

**Figure 9: The transient energy consumption for gold and carbon black nanofluids.**
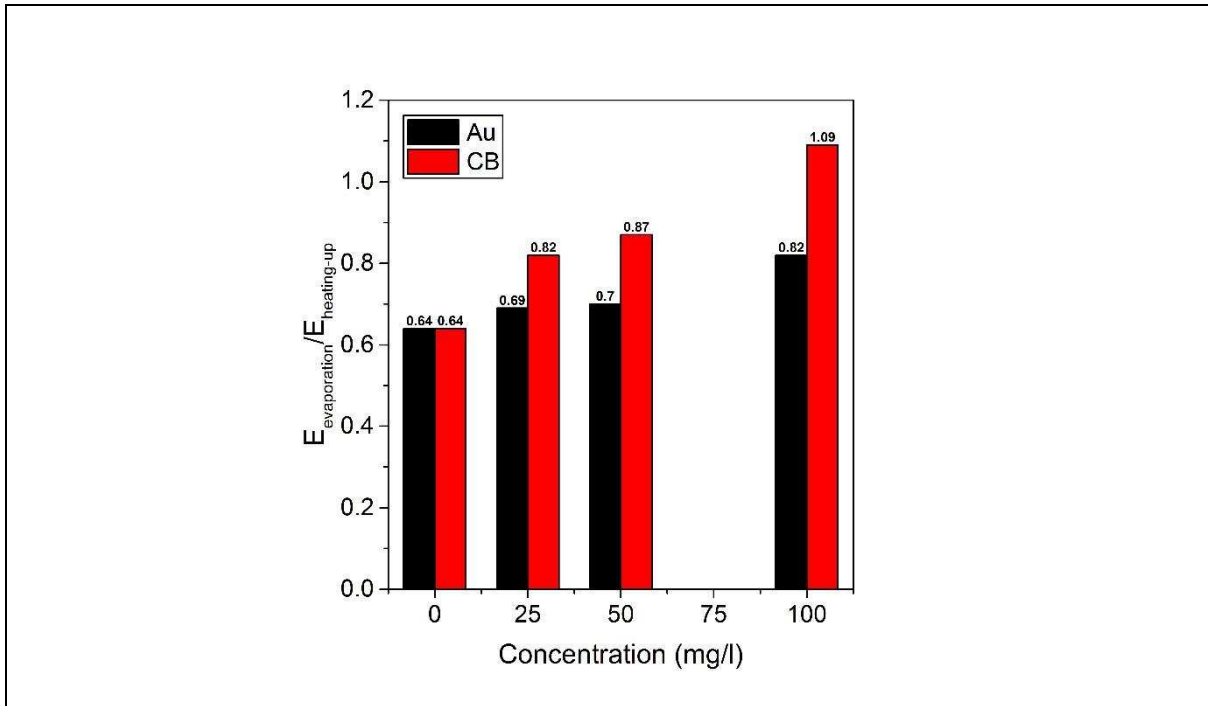
Figure 10: The ratio of energy consumed by evaporation to the energy stored in the nanofluids at time= 600 s.